Climatology of GNSS ionospheric scintillation at high latitudes

L. Spogli[(1)], L. Alfonsi[(1)], G. De Franceschi[(1)], V. Romano[(1,2)], M. H. O. Aquino[(2)], A. Dodson[(2)]

[1]Istituto Nazionale di Geofisica e Vulcanologia (INGV), Via di Vigna Murata, 605, 00143 Rome, Italy.

[2]Institute of Engineering Surveying and Space Geodesy (IESSG), University Park Nottingham, NG7 2RD, Nottingham, United Kingdom.

Email: luca.spogli@ingv.it

ABSTRACT

We analyse GNSS ionospheric scintillation data in the polar areas of both hemispheres to develop a climatology over a large geomagnetic quiet period. The conditions of the near-Earth environment leading to scintillation scenarios are investigated via scintillation occurrence. Within this scope we realize maps of scintillation occurrence as a function of the magnetic local time (MLT) and of the altitude adjusted corrected geomagnetic coordinates (AACGM). The maps are realized merging observations from a network of four GISTM (GPS Ionospheric Scintillation and TEC Monitor) in the Northern Europe and two GISTM in Antarctica during the year 2008. The results highlight the possibility to investigate the impact of ionospheric irregularities on the phase and amplitude of GNSS signals, evidencing the auroral and cusp/cap contributions. This works aims to contribute to development of nowcasting and forecasting tools for GNSS ionospheric scintillation.

1. INTRODUCTION

Under perturbed conditions caused by intense solar wind-magnetosphere coupling, the ionosphere may become highly turbulent and the probability of irregularities formation, typically enhancements or depletions of the electron density embedded in the ambient ionosphere, increases. Such irregularities cause diffraction effects, mainly due to the random fluctuations of the refractive index of the ionosphere, on the satellites signals passing through them and consequent perturbations may cause GNSS navigation errors and outages, abruptly corrupting its performance [1]. Due to the morphology of the geomagnetic field, whose lines are almost vertical at high latitude, polar areas are characterized by a significant presence of ionospheric irregularities, having scale sizes ranging from hundreds of kilometres down to a few centimetres and with highly dynamic structures. The understanding and consequent mitigation of the effect of such phenomena is important, especially in view of the current solar cycle (24), whose maximum is expected in 2012, and of the forthcoming launch of the Galileo system.

We analyse the fluctuations in the carrier frequency of the radio waves received on the ground, commonly referred to as ionospheric amplitude and phase scintillations, to investigate the physical processes causing them and, conversely, to understand how these processes affect the operational capabilities of GNSS receivers under different geomagnetic conditions. The phase scintillations on GNSS signals are likely caused by ionospheric irregularities of scale size of hundreds of meters to few kilometres. The amplitude scintillations on GNSS signals are caused by ionospheric irregularities of scale size smaller than the Fresnel radius, which is of the order of hundreds of meters for GNSS signals. The results, obtained by statistically analyzing a large data sample over a wide period, show the effect of ionospheric disturbances on GNSS signals, evidencing the different contributions of the auroral and the cusp/cap ionosphere.

2. SCINTILLATION RECEIVERS NETWORK

The Istituto Nazionale di Geofisica e Vulcanologia (INGV) and the Institute of Engineering Surveying and Space Geodesy (IESSG) of the University of Nottingham manage the same kind of GISTM (GPS Ionospheric Scintillation and TEC Monitor) receivers over the European high and mid latitude regions and over Antarctica. The GISTM receivers consist of NovAtel OEM4 dual-frequency receivers with special firmware specifically able to compute in near real time the widely used amplitude and the phase scintillation indices from the GPS L1 frequency signals, and the ionospheric TEC (Total Electron Content) from the GPS L1 and L2 carrier

phase signals. These indices are both based on 50 Hz measurements at L1 frequency [2]. From this ground-based network, we are able to capture the dynamics of ionospheric plasma in a wide latitudinal range, from auroral to cusp/cap regions, considering the contribution of both hemispheres, in a bi-polar framework. In particular, the stations considered in our analysis are located at Ny-Ålesund (78.9°N, 11.9°E), Longyearbyen (78.2°N, 16.0°E), Trondheim (63.4°N, 10.4°E) and Nottingham (52.9°N, 1.2°W) in the Northern hemisphere and at Mario Zucchelli Station (74.7°S, 164.1°E) and Concordia Station (75.1°S, 123.2°E) in Antarctica. The data collection starts in 2001 up to now. Tab. 1 shows the geographic and corrected geomagnetic coordinates of the stations, together with the receivers identifier (ID) and geographical location.

3. DATA AND METHOD

We analyze the scintillation indices computed over 60 seconds data acquired during 2008. The data sets show very few gaps: the percentage of available days of data, averaged over the six stations, is 84.3%, i.e. about 308.5 days. To reduce the impact of non-scintillation related tracking errors, only indices derived from observations at an elevation angle greater than 15° are considered. Scintillation indices are projected to the vertical according to the following formulae:

$$\sigma_\varphi(\alpha_{elev} = 90^o) = \sigma_\varphi(\alpha_{elev}) \sin^a(\alpha_{elev}) \quad (1)$$

$$S_4(\alpha_{elev} = 90^o) = S_4(\alpha_{elev}) \sin^b(\alpha_{elev}) \quad (2)$$

where α_{elev} is the elevation angle, $\sigma_\varphi(\alpha_{elev})$ and $S_4(\alpha_{elev})$ are the indices measured by the receivers at a given elevation angle, along the path between satellite and receiver. According to [3],[4] and as described in [6], *a* is assumed to be equal 0.5, while *b* is assumed to be equal to 0.9. Hereafter the indices refer to their vertically projected values. Merging the information from the northern hemisphere stations (NYA1, LYB0, NSF1 and NSF6) and, separately, from their southern counterparts (DMC0 and BTN0), we construct maps of percentage of occurrence of the scintillation indices in Altitude Adjusted Corrected Geomagnetic Coordinates (AACGM) [5]: Magnetic Latitude (M_{lat}) vs Magnetic Local Time (MLT). The percentage of occurrence is evaluated for each bin of 3h MLT x 2° M_{lat}, as:

$$\frac{N(S_4 \text{ or } \sigma_\varphi > threshold)}{N_{tot}} \quad (3)$$

where $N(S_4$ or $\sigma_\varphi >$ threshold) is the number of data points corresponding to a scintillation index above a given threshold, while N_{tot} is the total number of data points in the bin. Accordingly to [6], the selected thresholds are 0.25 radians for σ_φ and 0.25 for S_4 and the selected accuracy has to be lower than 2.5%, in order to exclude the contribution of bins with poor statistics.

4. GEOMAGNETIC CHARACTERIZATION

The period investigated is characterized by quiet geomagnetic conditions, so it can be useful for our climatological purpose. The K_p index, as provided by the World Data Center for Geomagnetism of Kyoto, is used in this paper to define the geomagnetic behaviour of a particular day. We define a day as quiet if every K_p value is strictly less than 5 and if 50% of values in that day is less than or equal to 4. According to this assumption only 18 days are found to be disturbed (5% of the whole year). By consequence scintillation maps referring to disturbed days are much less populated than the ones referring to quiet days. Nevertheless, the proposed threshold, introduced in Sect. 3, ensures the consistency between the two kinds of maps.

5. OBSERVATION AND DISCUSSION

Fig. 1 shows the maps of phase scintillation (σ_φ) percentage of occurrence for both hemispheres and during quiet and disturbed days, while the corresponding maps of amplitude scintillation (S_4) are shown in Fig.2. The comparison between amplitude and phase scintillation occurrence indicates that polar areas are much more sensitive to phase than to amplitude scintillation, confirming what was already found in [7]. The scintillation maps describe clearly also the different field of view of the stations in the two hemispheres: the European receivers cover a very wide range in M_{lat}, from mid to cusp/cap latitudes, while the two stations in Antarctica are mainly at cap latitudes, except for few hours of the day in which BTN0 is located close to the cusp position [8]. As expected the scintillation occurrence is at lower levels than the ones during October/November 2003, as shown in [6], which was a very disturbed period indeed, characterized by two great magnetic storms.

Concerning the phase scintillation maps (Fig.1), there is no strong characterization of the midnight and noon sector during the quiet days for both hemispheres, while the disturbed days pattern shows levels of scintillation occurrence similar to those found in 2003, according to [6]. The disturbed days of 2008 over the northern hemisphere show a characterization around 75° M_{lat} for every MLT, but especially around midnight and noon: this could be explained in terms of the position of the irregularities oval, defined as a modification of the auroral oval in which the irregularities causing scintillations should be confined [9]. Concerning the disturbed days over the southern hemisphere a typical cusp effect in the pre-noon sector is evident, due to the contribution of the BTN0 receiver [8], not shown here.

Concerning the amplitude scintillation maps, the comparison between quiet and disturbed days over the northern hemisphere shows a broader MLT area of

scintillation around 50° M_{lat} and a weak enhancement of S_4 occurrence in the pre-midnight sector under perturbed conditions. This could be due to the higher degree of variability of the irregularities region. The southern hemisphere maps of amplitude scintillation show an almost negligible occurrence, likely due to a field of view mainly covering the polar cap area.

6. SUMMARY AND CONCLUSIONS

In this analysis we constructed maps of occurrence of scintillation indices as a function of the altitude adjusted geomagnetic latitude and magnetic local time. Within this scope, we analyse data taken along 2008 by six GISTM receivers located both in Northern Europe and Antarctica. The receivers cover a wide range of latitude: from mid to cusp/cap latitudes in the northern hemisphere, and mainly cap latitudes in the southern hemisphere. The aim of the study is to develop a scintillation climatology over both polar areas along a very quiet geomagnetic period, as in the case of 2008.
The maps are realized for both hemispheres and for quiet and disturbed geomagnetic conditions, defined via the Kp index. There were only 18 disturbed days in the analyses, meaning about 5% of the whole year.

This work confirms that polar areas of the ionosphere are much more sensitive to phase than to amplitude scintillation. The maps show no particular characterization during quiet days. During the disturbed days the northern hemisphere shows a characterization likely due to the position of the irregularities region, while the southern hemisphere shows a typical cap effect. For what concerns amplitude scintillation, no contributions arise from the southern hemisphere, while in the northern hemisphere there are evident enhancements of scintillation occurrence possibly due to a higher degree of variability of the irregularities region.

7. ACKNOWLEDGEMENTS

The authors would like to thank Prof. Andrzej W. Wernik for his kind support and important comments and Dr. Cathryn Mitchell for her contribution in supporting the management of the Concordia receiver. The authors also thank the Programma Nazionale di Ricerche in Antartide (PNRA), CNR (Consiglio Nazionale delle Ricerche), the World Data Center for Geomagnetism of Kyoto, the Engineering and Physical Sciences Research Council of the UK (EPSRC) and the Royal Society.

8. REFERENCES

1. Committee on the Societal and Economic Impacts of Severe Space Weather Events: Severe Space Weather Events - Understanding Societal and Economic Impacts Workshop Report, ISBN: 0-309-12770-X, 2008.
2. Van Dierendonck, A. J., Klobuchar, J. and Hua, Q.: Ionospheric scintillation monitoring using commercial single frequency C/A code receivers, in: ION GPS-93 Proceedings of the Sixth International Technical Meeting of the Satellite Division of the Institute of Navigation, Salt Lake City, U.S.A., 22-24 September, 1333–1342, 1993.
3. Rino, C. L.: A power law phase screen model for ionospheric scintillation. I-Weak Scatter. II – Strong scatter. Radio Sci., 14, 1135-1145 and 1147-1155, 1979.
4. Wernik A.W., Secan, J. A., Fremouw, E. J.: Ionospheric irregularities and scintillation, Adv. Space Res., 31, 4, 971-981, 2003.
5. Baker, K.B. and Wing, S.: A new magnetic coordinate system for conjugate studies at high latitudes, J. Geophys. Res., 94, 9139-9143, 1989.
6. Spogli, L., Alfonsi, Lu., De Franceschi, G., Romano, V., Aquino, M.H.O., Dodson, A.: Climatology of GPS Ionospheric Scintillations over the Auroral and Cusp European Regions, submitted to Annales Geophysicae.
7. Meggs, R. W., Mitchell, C. N., Honary, F.: GPS scintillation over the European Arctic during the November 2004 storms, GPS Solut., 12, 281–287, doi:10.1007/s10291-008-0090-3, 2008.
8. Lepidi, S., Francia, P., Villante, U., Meloni, A., Lazarus, A.J., Lepping, R.P.: The Earth's passage of the April 11, 1997 coronal ejecta: geomagnetic field fluctuations at high and low latitude during northward interplanetary magnetic field conditions. Ann. Geophysicae 17, 1245-1250, 1999.
9. Aarons, J. (1997), Global Positioning system phase fluctuations at auroral latitudes, J. Geophys. Res., 102, A8, 17,219-17,231.

ID	Location	Latitude	Longitude	CGLat	CGLon
NYA1	Ny-Ålesund	78.9°N	11.9°E	76.0°N	112.3°E
LYB0	Longyearbyen	78.2°N	16.0°E	74.7°N	129.2°E
NSF1	Trondheim	63.4°N	10.4°E	60.7°N	91.4°E
NSF6	Nottingham	52.9°N	1.2°W	54.8°N	87.1°E
DMC0	Concordia Station	75.1°S	123.2°E	84.4°S	222.6°E
BTN0	Mario Zucchelli Station	74.7°S	164.1°E	77.1°S	275.9°E

Table 1. Geographic and corrected geomagnetic coordinates (CGLat, CGLon) of the GISTM receivers, together with receivers identifier (ID) and geographical location.

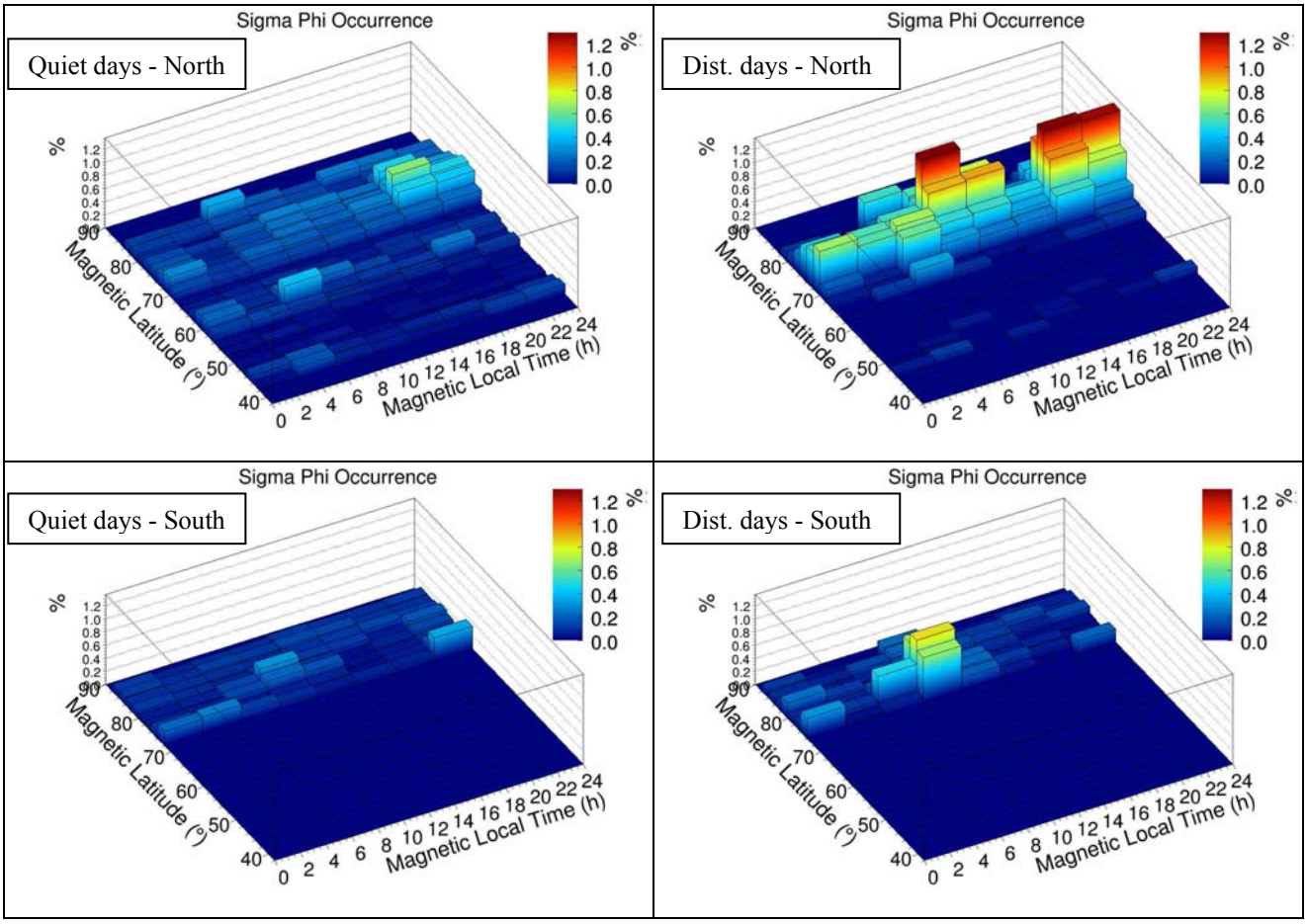

Figure 1. Maps of σ_φ percentage of occurrence. Upper row: northern hemisphere quiet days (left map) and disturbed days (right map). Lower row: southern hemisphere quiet days (left map) and disturbed days (right map).

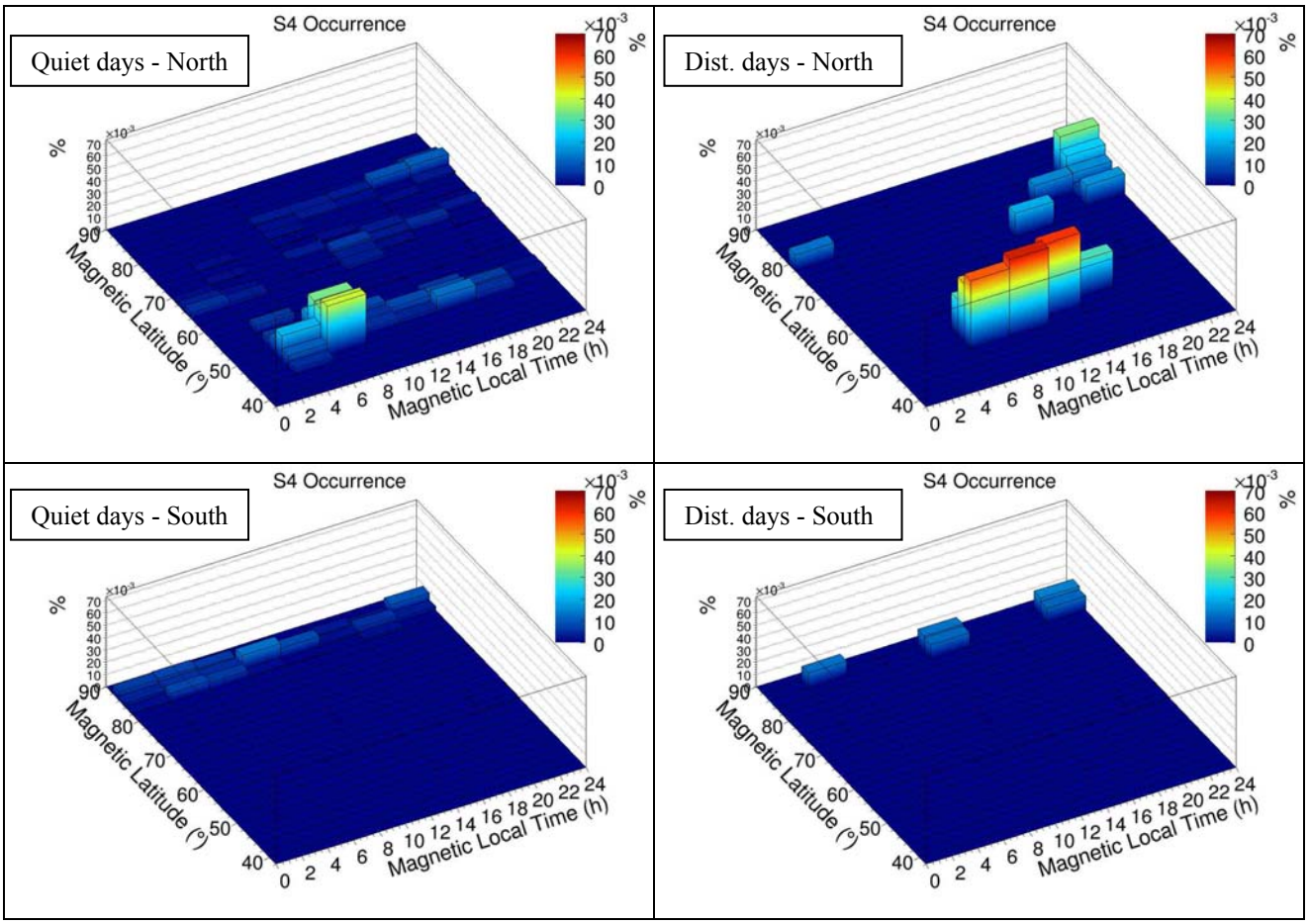

Figure 2. Maps of S_4 percentage of occurrence. Upper row: northern hemisphere quiet days (left map) and disturbed days (right map). Lower row: southern hemisphere quiet days (left map) and disturbed days (right map).